

# A Mathematical Model of the Magnetic Field in the Magnetic Circuit Window of the Transformer Converter on the Basis of Poisson and Laplace Differential Equations

**Marinka Baghdasaryan**

Institute of Energetics and Electrical Engineering, National Polytechnic University of Armenia, Armenia  
m.baghdasaryan@seua.am (corresponding author)

**Gor Vardanyan**

Institute of Energetics and Electrical Engineering, National Polytechnic University of Armenia, Armenia  
gor.vardanyan@polytechnic.am

*Received: 31 January 2025 | Revised: 20 February 2025 and 24 February 2025 | Accepted: 27 February 2025*

*Licensed under a CC-BY 4.0 license | Copyright (c) by the authors | DOI: <https://doi.org/10.48084/etasr.10391>*

## ABSTRACT

The technical and economic requirements for electrical devices are increasing, mainly aiming at ease of operation, increased efficiency and measurement accuracy, as well as cost reduction. These requirements can be met by conducting a comprehensive study of the components of each designed device and their characteristics. For a contactless current meter, which has found wide application in the power system, meeting the above requirements is of particular interest. However, it is impossible to achieve this without putting forward new approaches to the current converter study. Since the output signal of the current converter mainly depends on the position of the conductive conductor in the magnetic circuit window and on the structural parameters of the magnetic circuit, a new modeling approach is proposed in this paper. Analytical dependencies have been obtained which, unlike known analogues, allow one to evaluate the magnetic field image without discretizing the observed area, as well as by entering the initial values of the potential. The proposed dependencies allow the determination of the characteristic parameters of the field at any position of the conductor, while in the case of known methods it is necessary to discretize the observed area again for each new position, which leads to additional difficulties.

*Keywords-current converter; magnetic circuit; magnetic field; transformer converter*

## I. INTRODUCTION

The development of electric power systems, automatic control and monitoring systems, radio electronics, automation, as well as several branches of new technology, brought to the fore the need for contactless measurement and subsequent transmission to process the data on currents flowing in busbars. During electrical equipment operation, in most cases, current measurements should be carried out without breaking the circuits to prevent equipment downtime, eliminate emergency situations, and ensure safety measures for the operating personnel [1-3]. For the contactless measurement of current values from several fractions of an ampere to several kilo amperes, Contactless Current Measuring Devices (CCMDs) are successfully used. CCMD operation is based on the measured current conversion. According to the conversion method, CCMDs are divided into two main groups, as illustrated in Figure 1:

- Converters with direct conversion, which are categorized into those with an auxiliary power source and those without.
- Converters with balancing conversion.

In CCMDs of direct conversion with an auxiliary power source, magneto resistors or Hall-sensors are used [4, 5]. A converter based on the Hall-effect (galvanomagnetic), with the introduction of compensation, allows for the necessary range of currents. The disadvantage of these converters, though, is the need to introduce compensation with large power consumption and, consequently, the former's lack of autonomous operation, since it must be powered by an industrial network. CCMSs of direct conversion without an auxiliary power source in turn, are distinguished according to the operating principle, into electromagnetic and transformer (inductive). CCMDs based on an electromagnetic converter are characterized by their simple design and are based on the force action of the measured current. The main disadvantage of an electromagnetic converter

is the need to place it in a certain fixed position relative to the measured conductor during each measurement. In addition, the presence of a large dependence of the output signal on the effect of an external magnetic field and the difficulties associated with providing a multi-limit measurement scale are significant. Transformer converters have become more widespread due to their remarkable combination of simple design and wide metrological capabilities. The main drawback of a transformer converter is the dependence of the output signal on the position of the measured conductor in the window of the magnetic circuits. Comparative analysis showed that regarding the accuracy of parameter stability, ease of operation, power consumption, wide measurement range, and design simplicity, the most promising are transformer converters, the study of which is the aim of the current work. At present, a wealth of experimental and theoretical material has been accumulated, allowing the study of the electromagnetic characteristics of transformer converters [6-16], however, there is no unified methodology for assessing their electromagnetic characteristics. A comprehensive study of the electromagnetic characteristics of transformer converters was carried out in [17-19].

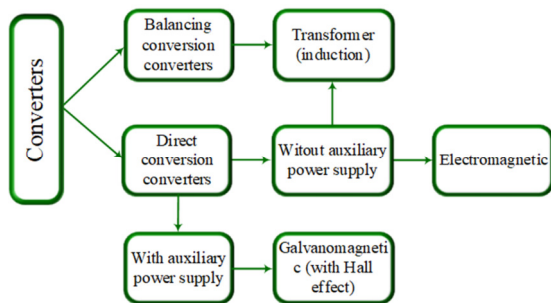


Fig. 1. Classification of current converters.

Authors in [20, 21] analyzed the parameters of the magnetic part of the equivalent circuit of a current transformer in the frequency range of 50 Hz to 5 kHz. The conducted tests make it possible to understand the obtained values of the frequency characteristics of the current error and the phase shift of the corrected inductive current transformer. It should be noted that for a comprehensive assessment of current converters, it is necessary to study the magnetic field distribution in the magnetic circuit window. Therefore, numerical methods for obtaining an image of the magnetic field distribution have become increasingly popular [22-24]. Their advantage is that they can obtain characteristic parameters of the field of any complex structure and boundary conditions with a given accuracy [23, 25]. Considering the magnetic field modeling, the use of a hybrid model of Finite Difference (FD) and Finite Element (FE) methods [23] is of particular interest. This model is first discretized in the form of rectangular blocks and divided into FD and FE zones, increasing calculation accuracy, as well as its duration. Despite the widespread use of numerical methods, their utilization is not always advisable. The main disadvantage of the former is that the solution must be completely repeated for each new set of parameters of a given problem. That is, when calculating the field deploying a numerical method, the values of the function characterizing the

field are obtained only for one set of parameter values. For new parameter values to be obtained, the process must be repeated. To avoid this drawback, it is often necessary to use analytical equations to determine the field potential. The research carried out toward this direction is valuable and has important practical significance for studying the magnetic characteristics of electromagnets of various configurations. However, they are aimed at solving individual specific problems. Considering that the result of the evaluation of the electromagnetic parameters of transformer converters used in the CCMDs significantly depends on the position of the current-carrying wire in the magnetic circuit window and the cross-sectional area, it is, therefore, necessary to develop a mathematical model for studying the magnetic field in the magnetic circuit window.

The aim of this work is to develop a mathematical model of the magnetic field, which will allow studying the magnetic characteristics of transformer converters for measured conductors of different cross-sections and any position of the magnetic wire in the window, as well as for various dimensional data of the magnetic wire.

## II. METHODOLOGY

### A. Statement of the Problem and Methodology Justification

The study and calculation of magnetic fields in the window of the magnetic circuit of a transformer converter is a rather complex and labor-intensive task, since the magnetic circuit has a three-dimensional shape and the current changes over time. If the problem is considered static, then it is practically impossible to find an analytical function of three unknown arguments. Thus, such assumptions must be accepted, under which the magnetic field is determined with sufficient accuracy by two parameters in a two-coordinate system. The results of the analysis and calculation of magnetic fields of the magnetic circuit of a transformer converter mainly depend on the field excitation method, the shape and properties of the surfaces limiting field propagation, and the configuration of the cross-section of the conductor with the measured current. To simulate the magnetic field in the window of the magnetic circuit of the transformer converter, the following assumptions are made:

- The steel of the magnetic circuit has an infinitely large magnetic permeability.
- The measured current is distributed over the cross-section of the conductor with a uniform density.
- The magnetic field has a plane-parallel configuration.

The problem can be set as follows: Determine the distribution pattern of the magnetic field in the magnetic circuit window ( $0 \leq x \leq a$ ,  $0 \leq y \leq b$ ), created with the measured current and located at point  $x=x_0$ ,  $y=y_0$  (Figure 2). The magnetic field pattern depends primarily on the geometric shape and cross-section of the current-carrying conductor. The field excited by a conductor (bus) of circular and rectangular cross-sections is of practical interest. A great amount of research has been devoted to determining the magnetic induction of a conductor (bus) of rectangular cross-section [26]. Hence, in this paper, attention is paid to a conductor of circular cross-section with radius  $R$ .

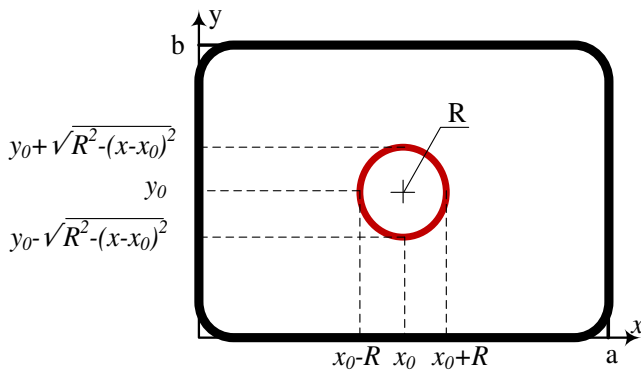


Fig. 2. The distribution pattern of the magnetic field in the magnetic circuit window.

**B. The Proposed Algorithm**

In the space between the halves of the magnetic circuit (in the window of the magnetic circuits), the vector potential  $A(x, y)$  satisfies the Poisson equation [27, 28], which determines the field in the region where the current flows (the location of the conductor with the measured current), and the Laplace equation, which determines the field in the region where the current does not flow. In this case, the problem can be reduced to solving the Poisson equation in Cartesian coordinates, considering the condition:

$$\frac{d^2 A}{dx^2} + \frac{d^2 A}{dy^2} = -\mu_0 \cdot j(x, y), \tag{1}$$

$$j(x, y) = \begin{cases} j & \text{at } (x-x_0)^2 + (y-y_0)^2 \leq R^2 \\ 0 & \text{at } (x-x_0)^2 + (y-y_0)^2 > R^2 \end{cases} \tag{2}$$

where  $R$  is the radius of the measured current conductor,  $(x_0, y_0)$  are the coordinates of the position of the current-carrying conductor,  $\mu_0$  is the Magnetic permeability,  $j$  is the current density, and  $A$  is the vector potential  $A(x,y)$  [26], given by:

$$A(x, y) = \sum_{n=1}^{\infty} X_n(x) Y_n(y) \tag{3}$$

Considering that the magnetic field under investigation has infinitely large magnetic permeability, the limiting conditions can be presented by:

$$\text{at } y = 0 \rightarrow \frac{dA}{dy} = 0 \tag{4}$$

$$\text{at } y = b \rightarrow \frac{dA}{dy} = 0 \tag{5}$$

$$\text{at } x = 0 \rightarrow \frac{dA}{dx} = 0 \tag{6}$$

$$\text{at } x = a \rightarrow \frac{dA}{dx} = 0 \tag{7}$$

The expression  $Y_n(y)$  is determined from the solution of a second-order differential equation considering the limiting conditions (4) and (5) and has the form:

$$Y_n(y) = \cos \frac{n\pi}{b} y \tag{8}$$

where  $n$  is the period of the function.

To calculate  $X_n(x)$ , (8) is used in (3) and after integration over  $y$ , within a range of 0 to  $b$ , (9) is given:

$$X_n(x) = \frac{2}{b} \int_0^b A(x, y) \cos \frac{n\pi}{b} y dy \tag{9}$$

Then, by multiplying (1) by the right-hand side of (8) and integrating over  $y$ , within a range of 0 to  $b$ , (10) is obtained:

$$\begin{aligned} & \int_0^b \frac{\partial^2 A(x, y)}{\partial x^2} \cos \frac{n\pi}{b} y dy + \\ & + \int_0^b \frac{\partial^2 A(x, y)}{\partial y^2} \cos \frac{n\pi}{b} y dy = \\ & = \mu_0 \int_0^b j(x, y) \cos \frac{n\pi}{b} y dy \end{aligned} \tag{10}$$

Calculating the integrals:

$$\int_0^b \frac{\partial^2 A(x, y)}{\partial x^2} \cos \frac{n\pi}{b} y dy = \frac{b}{2} \frac{d^2 X_n(x)}{dx^2} \tag{11}$$

$$\int_0^b \frac{\partial^2 A(x, y)}{\partial y^2} \cos \frac{n\pi}{b} y dy = -\frac{(n\pi)^2}{2b} X_n(x) \tag{12}$$

and using them in (10), it is obtained:

$$\begin{aligned} X_n''(x) - \left(\frac{n\pi}{b}\right)^2 X_n(x) &= \\ = -\frac{2}{b} \mu_0 \cdot \psi(x) \cdot \int_c^d \cos \frac{n\pi}{b} y dy \end{aligned} \tag{13}$$

where:

$$c = y_0 - \sqrt{R^2 - (x-x_0)^2}, \quad d = y_0 + \sqrt{R^2 - (x-x_0)^2}, \quad \text{and}$$

$$\psi(x) = \begin{cases} j & \text{at } (x-x_0)^2 + (y-y_0)^2 \leq R^2 \\ 0 & \text{at } (x-x_0)^2 + (y-y_0)^2 > R^2 \end{cases} \tag{14}$$

Considering (14) and after integrating, (13) becomes:

$$X_n''(x) - \left(\frac{n\pi}{b}\right)^2 X_n(x) = -j\mu_0 \frac{4}{n\pi} \cos\left(\frac{n\pi}{b} y_0\right) \cdot \sin\left(\frac{n\pi}{b} \sqrt{R^2 - (x-x_0)^2}\right) \cdot [H(x-(x_0-R)) - H(x-(x_0+R))]$$

where:

$$[H(x-(x_0-R)) - H(x-(x_0+R))],$$

is the Heaviside decomposition.

Setting  $g_1$  and  $\Delta(x_0, x, R)$  as follows:

$$g_1 = \sin\left(\frac{n\pi}{b} \sqrt{R^2 - (x-x_0)^2}\right),$$

$$\Delta(x_0, x, R) = [H(x-(x_0-R)) - H(x-(x_0+R))],$$

the solution of (15) is represented by:

$$X_n(x) = C_1(x) ch \frac{n\pi}{b} x + C_2(x) sh \frac{n\pi}{b} x \tag{16}$$

Using the method of variation of constants [29] for  $C_1(x)$  and  $C_2(x)$ , the following equations are obtained:

$$C_1(x) = g_2 \int_0^x g_1 \Delta(x_0, x, R) sh\left(\frac{n\pi}{b} x\right) dx + C_1 \tag{17}$$

$$C_2(x) = g_2 \int_0^x g_1 \Delta(x_0, x, R) ch\left(\frac{n\pi}{b} x\right) dx + C_2$$

where:

$$g_2 = j\mu_0 \frac{4b}{(n\pi)^2} \cos\left(\frac{n\pi}{b} y_0\right).$$

Therefore, by using (17) in (16) the solution is given by:

$$X_n(x) = C_1 ch \frac{n\pi}{b} x + C_2 sh \frac{n\pi}{b} x - g_1 \int_0^x K_2 K_4 \Delta(x_0, x, R) d\eta \tag{18}$$

where:

$$K_2 = \sin\left(\frac{n\pi}{b} \sqrt{R^2 - (\eta-x_0)^2}\right) \text{ and } K_4 = sh \frac{n\pi}{b} (x-\eta).$$

The integration constants  $C_1$  and  $C_2$ , are calculated from the boundary equations for the function  $A(x, y)$ :

Setting  $x=0$  and  $x=a$ , gives:

$$X_n'(0) = 0 \tag{19}$$

$$X_n'(a) = 0 \tag{20}$$

From (19),  $C_2=0$  is calculated, and from (20) we get:

$$C_1 = \frac{g_1}{sh\left(\frac{a}{b} n\pi\right)} \cdot \int_{x_0-R}^{x_0+R} K_2 ch \frac{n\pi}{b} (a-\eta) d\eta$$

So, the solution  $X_n(x)$  is given by:

$$X_n(x) = -g_1 \cdot [K_2 K_4 \Delta(x_0, x, R) - \int_0^x \frac{ch\left(\frac{n\pi}{b} x\right)}{sh\left(\frac{n\pi}{b} a\right)} d\eta \cdot \int_{x_0-R}^{x_0+R} K_2 ch \frac{n\pi}{b} (a-\eta) d\eta] \tag{21}$$

### III. RESULTS AND DISCUSSION

#### A. Estimation of the Magnetic Field Distribution

The vector potential of the magnetic field can be obtained from (3), (8) and (21), because of the integrated application of the Laplace and Poisson differential equations. The final expression of the magnetic potential using Heaviside decomposition [29] takes the form:

$$A(x, y) = -\sum_{n=1}^{\infty} K_1 \left[ \int_{x_0-R}^x K_2 K_4 d\eta + K_3 \int_{x_0-R}^{x_0+R} K_2 K_5 d\eta \right] \tag{22}$$

$$A(x, y) = -\sum_{n=1}^{\infty} K_1 K_3 \int_{x_0-R}^{x_0+R} K_2 K_5 d\eta \tag{23}$$

$$A(x, y) = -\sum_{n=1}^{\infty} K_1 \left[ \int_{x_0-R}^{x_0+R} K_2 K_4 d\eta + K_3 \int_{x_0-R}^{x_0+R} K_2 K_5 d\eta \right] \tag{24}$$

where:

$$K_1 = \mu_0 j \frac{4b}{(n\pi)^2} \cos\left(\frac{n\pi}{b} y_0\right) \cos\left(\frac{n\pi}{b} y\right),$$

$$K_3 = \frac{ch \left( \frac{n\pi}{b} x \right)}{sh \left( \frac{n\pi}{b} a \right)}, K_5 = ch \left( \frac{n\pi}{b} (a - \eta) \right)$$

Based on analytical dependencies and calculation results for different positions of the conductor with the measured current, the four following field distribution patterns were constructed for a round conductor with different cross-section sizes: Two distribution patterns of the magnetic field in the window of the magnetic circuit were created by a current-carrying conductor with a conductor cross-section of 0.8 cm<sup>2</sup>, one for the position of the current-carrying conductor for coordinates x<sub>0</sub>=2, y<sub>0</sub>=2, as depicted in Figure 3(a), and the other for the position of the current-carrying conductor for coordinates x<sub>0</sub>=3.5, y<sub>0</sub>=3.5, as portrayed in Figure 3(b). Then two other distribution patterns of the magnetic field in the window of the magnetic circuit were created by a current-carrying conductor with a cross-section of 12.5 cm<sup>2</sup>, one for the position of the current-carrying conductor for coordinates x<sub>0</sub>=2, y<sub>0</sub>=2, as displayed in Figure 4(a), and the other for the position of the current-carrying conductor for coordinates x<sub>0</sub>=3.5, y<sub>0</sub>=3.5, as shown in Figure 4(b).

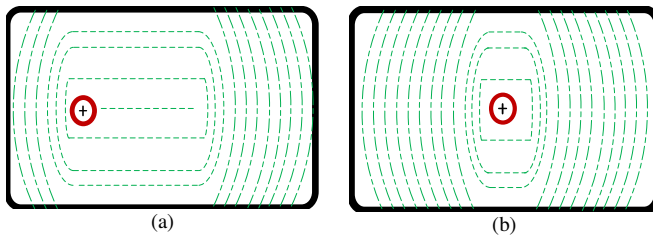


Fig. 3. Distribution patterns of the magnetic field with a conductor cross-section of 0.8 cm<sup>2</sup>.

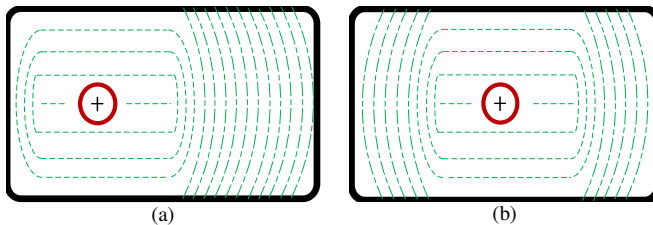


Fig. 4. Distribution patterns of the magnetic field with a conductor cross-section of 12.5 cm<sup>2</sup>.

All patterns used the algorithm presented in Figure 5, in the C Sharp software environment. The presented analytical dependencies make it possible to study the magnetic field at different positions and diameters of the conductor with the measured current. Having obtained the vector potential of the magnetic field, it is possible to determine the induction, which will make it possible to estimate the necessary electromagnetic parameters [30].

**B. Testing the Results**

The validity of the proposed model is verified by comparing it with the results of the finite increment method, used to calculate the magnetic field. The choice of this verification method is justified by the fact that to determine the

magnetic potential by the finite increment method, the differential equations characterizing the magnetic field (Poisson or Laplace) are replaced by a system of linear equations, which it is solved by a numerical method. A comparison of the analytical dependencies testing data for two cases, one with parameters: R=2 cm, j=159 A/cm<sup>2</sup>, x<sub>0</sub>=2, y<sub>0</sub>=2, as outlined in Table I, and the other with parameters: R=2 cm, j=159 A/cm<sup>2</sup>, x<sub>0</sub>=3.5, y<sub>0</sub>=3.5, as listed in Table II, with the results of the finite increment method, demonstrated that under homogeneous conditions, the difference in their potentials does not exceed 2%. A comparative analysis of the experiments conducted and the results exhibits that when using the methods considered, the maximum deviation of the changes in induction in the corresponding sections does not exceed 1.0%.

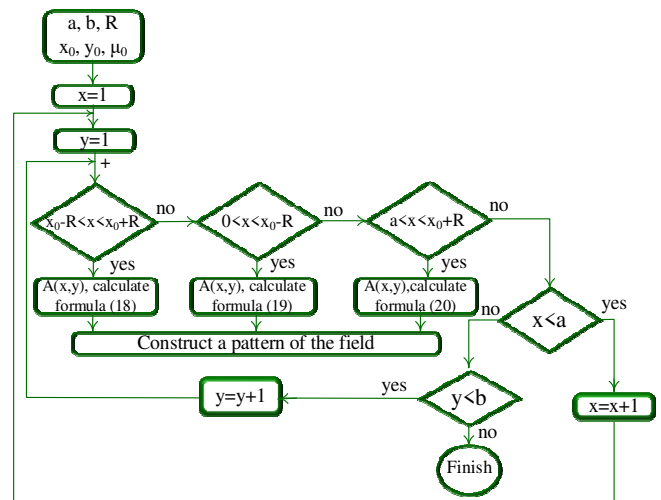


Fig. 5. Block diagram of the algorithm for determining the magnetic potential in the magnetic circuit window.

Figure 6 presents the changes in magnetic induction in the window of a magnetic circuit using the proposed model, while Figure 7 shows the changes in magnetic induction in the window of a magnetic circuit using the FD method.

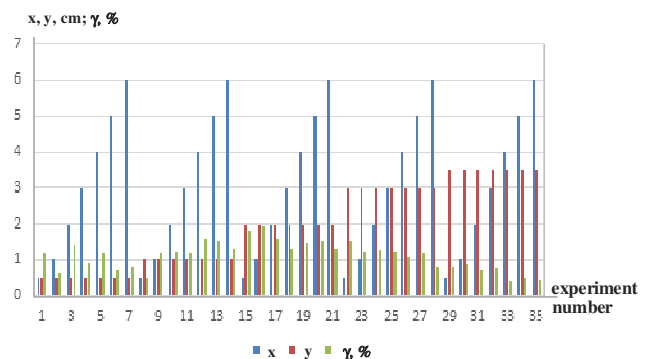


Fig. 6. Changes in magnetic induction using the proposed model.

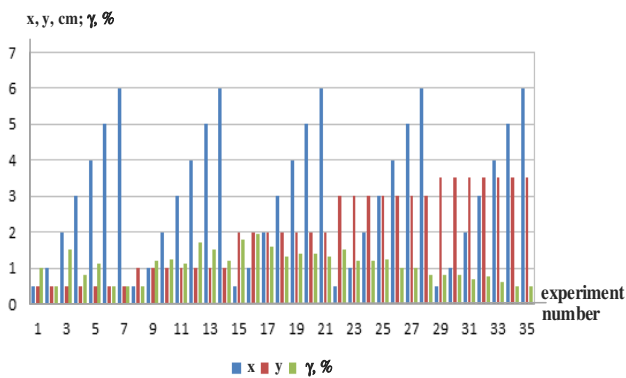


Fig. 7. Changes in magnetic induction using the FD.

TABLE I. TEST RESULTS FOR THE FIRST CASE

(x,y) cm	A(x,y) calculated by the proposed method	A(x,y) calculated by the FD method
(0.5,0.5), (0.5,3.5), (1.0,0.5), (1.0,3.5), (1.5,0.5), (1.5,3.5), (2.0,0.5), (2.0,3.5), (2.5,0.5), (2.5,3.5), (3.0,0.5), (3.0,3.5), (3.5,0.5), (3.5,3.5), (4.0,0.5), (4.0, 3.5), (4.5,0.5), (4.5,3.5)	4.271×10 <sup>-6</sup>	4.264×10 <sup>-6</sup>
(0.5,1.0), (0.5,3.0), (1.0,1.0), (1.0,3.0), (1.5,1.0), (1.5,3.0), (2.0,1.0), (2.0,3.0), (2.5,1.0), (2.5,3.0), (3.0,1.0), (3.5,1.0), (3.5,3.0), (4.0,1.0), (4.0,3.0)	1.208×10 <sup>-6</sup>	1.199×10 <sup>-6</sup>
(0.5,1.5), (0.5,2.5), (1.0,1.5), (1.0,2.5), (2.0,1.5), (2.0,2.5), (2.5,1.5), (2.5,2.5), (3.0,1.5), (3.0,2.5), (3.5,1.5), (3.5,2.5)	-3.467×10 <sup>-6</sup>	-3.459×10 <sup>-6</sup>
(0.5,2.0), (1.0,2.0), (1.5,2.0), (2.0,2.0), (2.5,2.0), (3.0,2.0), (3.5,2.0), (4.0,2.0)	-9.437×10 <sup>-6</sup>	-9.428×10 <sup>-6</sup>
(5.0,1.0), (5.0,3.0)	1.211×10 <sup>-6</sup>	1.208×10 <sup>-6</sup>
(5.5,1.0), (5.5,3.0)	1.224×10 <sup>-6</sup>	1.219×10 <sup>-6</sup>
(6.0,1.0), (6.0,3.0)	1.273×10 <sup>-6</sup>	1.288×10 <sup>-6</sup>
(6.5,1.0), (6.5,3.0)	1.527×10 <sup>-6</sup>	1.520×10 <sup>-6</sup>
(5.0,0.5), (5.0,3.5)	4.467×10 <sup>-6</sup>	4.459×10 <sup>-6</sup>
(5.5,0.5), (5.5,3.5)	4.702×10 <sup>-6</sup>	4.698×10 <sup>-6</sup>
(6.0,0.5), (6.0,3.5)	5.214×10 <sup>-6</sup>	5.206×10 <sup>-6</sup>
(6.5,0.5), (6.5,3.5)	6.314×10 <sup>-6</sup>	6.308×10 <sup>-6</sup>
(5.5,1.5), (5.5,2.5)	-3.896×10 <sup>-6</sup>	-3.885×10 <sup>-6</sup>
(4.5,3.0), (4.5,3.5)	4.360×10 <sup>-6</sup>	4.354×10 <sup>-6</sup>
(5.0,0.5), (5.0,3.5)	4.467×10 <sup>-6</sup>	4.454×10 <sup>-6</sup>
(5.5,0.5), (5.5,3.5)	4.702×10 <sup>-6</sup>	4.692×10 <sup>-6</sup>
(6.0,1.5), (6.0,2.5)	-4.407×10 <sup>-6</sup>	-4.400×10 <sup>-6</sup>

IV. CONCLUSIONS

Known studies on magnetic field modeling concern the solution of individual private problems, which limits the scope of their application. The models proposed by various authors for the magnetic circuit of contactless current meters are ineffective. This is mainly due to the fact that the current conductor creating the field can have a different cross-sectional area and be in different positions of the magnetic circuit window. In the current study, the authors propose a new analytical approach, which, unlike other methods, due to its simplicity and speed of application, is best applicable to

transformer converters used in contactless current meters. New analytical expressions for determining the magnetic field potential in the window of the winding wire of a current transformer were developed and proposed for further use. These expressions make it possible to obtain a picture of the field regardless of the geometric dimensions of the winding wire, the radius of the measured current conductor, the value of the current passing through it, and the position it occupies. As a result of their analysis, proposals are presented aimed at improving the device.

TABLE II. TEST RESULTS FOR THE SECOND CASE

(x,y) cm	A(x,y) calculated by the proposed method	A(x,y) calculated by the FD method
(1.5,1.0), (1.5,3.0), (2.0,1.0), (2.0,3.0), (2.5,1.0), (2.5,3.0), (3.0,1.0), (3.0,3.0), (3.5,1.0), (3.5,3.0), (4.0,1.0), (4.0,3.0)	2.869×10 <sup>-6</sup>	2.869×10 <sup>-6</sup>
(1.5,0.5), (1.5,3.5), (2.0,0.5), (2.0,3.5), (2.5,0.5), (2.5,3.5), (3.0,0.5), (3.0,3.5), (3.5,0.5), (3.5,3.5), (4.0,0.5), (4.0,3.5), (4.5,0.5), (4.5,3.5)	1.017×10 <sup>-5</sup>	1.021×10 <sup>-5</sup>
(1.5,1.5), (1.5,2.5), (2.0,1.5), (2.0,2.5), (2.5,1.5), (2.5,2.5), (3.0,1.5), (3.0,2.5), (3.5,1.5), (3.5,2.5)	-8.232.10 <sup>-6</sup>	-8.223.10 <sup>-6</sup>
(1.0,0.5), (1.0,1.5), (1.0,2.5)	-9.11×10 <sup>-10</sup>	-9.105×10 <sup>-10</sup>
(1.0,1.0), (1.0,3.0)	2.496×10 <sup>-14</sup>	2.481×10 <sup>-14</sup>
(0.5,0.5), (0.5,3.5), (0.5,1.5), (0.5,2.5)	-4.809×10 <sup>-10</sup>	-4.800×10 <sup>-10</sup>
(5.5,1.0), (5.5,3.0)	2.903×10 <sup>-6</sup>	2.896×10 <sup>-6</sup>
(6.0,1.0), (6.0,3.0)	3.030×10 <sup>-6</sup>	3.024×10 <sup>-6</sup>
(6.5,1.0), (6.5,3.0)	3.623×10 <sup>-6</sup>	3.601×10 <sup>-6</sup>
(0.5,1.0), (0.5,3.0)	5.403 ×10 <sup>-15</sup>	5.394 ×10 <sup>-15</sup>
(4.0,1.5), (4.0,2.5)	-8.370×10 <sup>-6</sup>	-8.361×10 <sup>-6</sup>
(5.0,1.5), (5.0,2.5)	-8.697×10 <sup>-6</sup>	-8.688×10 <sup>-6</sup>
(5.5,1.5), (5.5,2.5)	-9.254×10 <sup>-6</sup>	-9.243×10 <sup>-6</sup>
(5.5,0.5), (5.5,3.5)	1.110×10 <sup>-5</sup>	1.106×10 <sup>-5</sup>
(6.0,0.5), (6.0,3.5)	1.230×10 <sup>-5</sup>	1.237×10 <sup>-5</sup>
(5.0,0.5), (5.0,3.5)	1.060×10 <sup>-5</sup>	1.063×10 <sup>-5</sup>
(6.5,0.5), (6.5,3.5)	1.499×10 <sup>-5</sup>	1.482×10 <sup>-5</sup>

Unlike the widely used numerical methods in which the values of the function characterizing the field can be determined for only one set of parameter values, the proposed model avoids such limitations.

The current study's results make possible:

- The increase in the speed of obtaining a field image and its estimation due to a decrease in the discretization effect of the observed area, as well as the absence of a requirement for data on the initial value of the potential.
- The description of the nature of the magnetic field in the window of the magnetic circuit for its various dimensions, different positions of the measured current line, and different diameters.

The results obtained have a wide range of development possibilities. In particular, they can be used to evaluate the electromagnetic parameters of various electrical devices and

make decisions in accordance with the current standards, as well as to design new systems with improved performance.

## REFERENCES

- [1] P. Ripka, "Contactless measurement of electric current using magnetic sensors," *Technisches Messen*, vol. 86, no. 10, pp. 586–598, Oct. 2019, <https://doi.org/10.1515/teme-2019-0032>.
- [2] M. K. Baghdasaryan, *Methods of Research and Optimization of the Mineral Raw Material Grinding Process*. New York: Nova Science Pub Inc, 2019.
- [3] M. Baghdasaryan, A. Ulikyan, and A. Arakelyan, "Application of an Artificial Neural Network for Detecting, Classifying, and Making Decisions about Asymmetric Short Circuits in a Synchronous Generator," *Energies*, vol. 16, no. 6, Jan. 2023, Art. no. 2703, <https://doi.org/10.3390/en16062703>.
- [4] H. Su, H. Li, W. Liang, C. Shen, and Z. Xu, "Non-Contact Current Measurement for Three-Phase Rectangular Busbars Using TMR Sensors," *Sensors*, vol. 24, no. 2, Jan. 2024, Art. no. 388, <https://doi.org/10.3390/s24020388>.
- [5] K. T. Selva, O. A. Forsberg, D. Merkoulouva, F. Ghasemifard, N. Taylor, and M. Norgren, "Non-contact Current Measurement in Power Transmission Lines," *Procedia Technology*, vol. 21, pp. 498–506, Jan. 2015, <https://doi.org/10.1016/j.protcy.2015.10.034>.
- [6] F. Pranjić and P. Vrtič, "Development of Mathematical Models in Explicit Form for Design and Analysis of Axial Flux Permanent Magnet Synchronous Machines," *Applied Sciences*, vol. 10, no. 21, Jan. 2020, Art. no. 7695, <https://doi.org/10.3390/app10217695>.
- [7] M. Bezzubceva and V. Volkov, "Mathematical model for calculating the force field of loads in the magnetic liquefied layer of electromechanical dispersants," *E3S Web of Conferences*, vol. 279, 2021, Art. no. 03010, <https://doi.org/10.1051/e3sconf/202127903010>.
- [8] D. Lin and X. Chen, "Mathematical Models of 3D Magnetic Field and 3D Positioning System by Magnetic Field," *Applied Mathematics & Information Sciences*, vol. 8, no. 4, pp. 1647–1654, Jul. 2014, <https://doi.org/10.12785/amis/080420>.
- [9] G. G. Lazareva, I. P. Oksogoeva, and A. V. Sudnikov, "Mathematical Model of Matter Transfer in a Helical Magnetic Field Using Boundary Conditions at Infinity," *Journal of Mathematical Sciences*, vol. 285, no. 4, pp. 496–504, Nov. 2024, <https://doi.org/10.1007/s10958-024-07459-5>.
- [10] J. Ding, Y. Liu, S. Huang, H. Su, and L. Yao, "3-D Magnetic Field Mathematical Model Considering the Eccentricity and Inclination of Magnetic Gears," *IEEE Transactions on Magnetics*, vol. 60, no. 11, pp. 1–15, Aug. 2024, <https://doi.org/10.1109/TMAG.2024.3455796>.
- [11] Z. Amin and S. B. Sharif, "Use of integration to calculate the magnetic field in a space by using mathematica software for the effective production of nano-particles," *Journal of Interdisciplinary Mathematics*, vol. 25, no. 7, pp. 2007–2017, Oct. 2022, <https://doi.org/10.1080/09720502.2022.2133228>.
- [12] E. Paese, M. Geier, R. P. Homrich, and R. Rossi, "A coupled electric-magnetic numerical procedure for determining the electromagnetic force from the interaction of thin metal sheets and spiral coils in the electromagnetic forming process," *Applied Mathematical Modelling*, vol. 39, no. 1, pp. 309–321, Jan. 2015, <https://doi.org/10.1016/j.apm.2014.05.032>.
- [13] J. Swineburne, *The Measurement of Electric Currents: Electrical Measuring Instruments*. Palala Press, 2016.
- [14] T. Y. Kyaw, A. Torii, K. Doki, and A. Ueda, "Non-contact Current Measurement in Small Electric Parts by Using a Non-contact Thermometer," *IEEE Transactions on Electronics, Information and Systems*, vol. 124, no. 12, pp. 2470–2474, 2004, <https://doi.org/10.1541/ieej.iss.124.2470>.
- [15] B. D. Thanh and V. D. Quoc, "Computation and Evaluation of the Electromagnetic Parameters of Amorphous Core Transformers," *Engineering, Technology & Applied Science Research*, vol. 14, no. 1, pp. 12476–12481, Feb. 2024, <https://doi.org/10.48084/etasr.6359>.
- [16] A. Sadeghi, S. M. S. Barzegar, and M. Yazdani-Asrami, "A Simple and Fast Computation Equivalent Circuit Model to Investigate the Effect of Tape Twisting on the AC Loss of HTS Cables," *Engineering, Technology & Applied Science Research*, vol. 12, no. 1, pp. 8168–8174, Feb. 2022, <https://doi.org/10.48084/etasr.4382>.
- [17] G. Razin and A. Shchelkin, *Contactless measurement of electric currents*. Atomizdat, Moscow, 1974.
- [18] O. Portugall, S. Krämer, and Y. Skourski, "Magnetic Fields and Measurements," in *Handbook of Magnetism and Magnetic Materials*, M. Coey and S. Parkin, Eds. Cham: Springer International Publishing, 2020, pp. 1–70.
- [19] Y. Andreev and G. Abramzon, *Current converters for measurements without breaking the circuit*. (in Russian), Energiya, 1979.
- [20] E. Stano, P. Kaczmarek, and M. Kaczmarek, "Understanding the Frequency Characteristics of Current Error and Phase Displacement of the Corrected Inductive Current Transformer," *Energies*, vol. 15, no. 15, Jan. 2022, Art. no. 5436, <https://doi.org/10.3390/en15155436>.
- [21] S. E. Zocholl, *Analyzing and Applying Current Transformers*. Schweitzer Engineering Laboratories, Inc., 2004.
- [22] E. V. Karpukhin and A. N. Bormotov, "Numerical methods to calculate magnetic fields of magnetostriction level converter," *E3S Web of Conferences*, vol. 376, 2023, Art. no. 01101, <https://doi.org/10.1051/e3sconf/202337601101>.
- [23] W. Sarakorn and C. Vachiriatienchai, "Hybrid finite difference–finite element method to incorporate topography and bathymetry for two-dimensional magnetotelluric modeling," *Earth, Planets and Space*, vol. 70, no. 1, Jun. 2018, Art. no. 103, <https://doi.org/10.1186/s40623-018-0876-7>.
- [24] T. Chen, L. Wang, Y. Gu, and C. Tang, "Review on numerical analysis of electromagnetic characteristics for ferromagnetic wear debris," *The Journal of Engineering*, vol. 2019, no. 23, pp. 8715–8719, 2019, <https://doi.org/10.1049/joe.2018.9090>.
- [25] Z. Qi, X. Li, K. Fan, and Q. Zhi, "The three-dimensional finite element forward modelling of complex excitation source NMR," *Journal of Geophysics and Engineering*, vol. 17, no. 1, pp. 127–137, Feb. 2020, <https://doi.org/10.1093/jge/gxz096>.
- [26] K. J. Binns and P. J. Lawrenson, *Analysis and Computation of Electric and Magnetic Field Problems*, 2nd ed. Elsevier Science & Technology Books, 2013.
- [27] A. S. Demidov, *Equations of Mathematical Physics: Generalized Functions and Historical Notes*, 1st ed. Springer, 2023.
- [28] F. Mainardi, Ed., *Special Functions with Applications to Mathematical Physics*. MDPI, 2023.
- [29] M. A. B. Deakin, "Successive discoveries of the Heaviside expansion theorem," *International Journal of Mathematical Education in Science and Technology*, vol. 17, no. 1, pp. 51–60, Jan. 1986, <https://doi.org/10.1080/0020739860170107>.
- [30] P. J. Shepherd, *A Course in Theoretical Physics*, 1st ed. Chichester, West Sussex, United Kingdom: Wiley, 2013.